COLOUR COHERENCE OF SOFT GLUONS IN THE FULLY UNINTEGRATED NLO SINGLET KERNELS* **

M. Slawinska, A. Kusina, S. Jadach, M. Skrzypek

The Henryk Niewodniczański Institute of Nuclear Physics
Polish Academy of Sciences
Radzikowskiego 152, 31-342 Kraków, Poland

(Received May 6, 2011)

Feynman diagrams with two real partons contributing to the next-to-leading-order singlet gluon–quark DGLAP kernel are analysed. The infra-red singularities of unintegrated distributions are examined numerically. The analytical formulae are also given in some cases. The role of the colour coherence effects is found to be crucial for cancellations of the double- and single-logarithmic infra-red singularities.

DOI:10.5506/APhysPolB.42.1597
PACS numbers: 12.38.–t, 12.38.Bx, 12.38.Cy

1. Motivation

The study presented here is a part of the development of the fully exclusive next-to-leading order (NLO) Parton Shower Monte Carlo (MC) for precision QCD predictions for the LHC experiments, see [1,2,3]. DGLAP [4] evolution of parton distribution functions (PDFs) is modelled in the Monte Carlo within the unintegrated phase space. A methodology based on the collinear factorisation theorems in physical gauge based on Refs. [5] and [6] is used. MC program will simulate *exactly* NLO DGLAP evolution of PDFs by itself, as opposed to using pretabulated PDFs, provided by the non-MC programs like QCDNUM [7]. For the construction of such a new NLO parton shower MC program a new *exclusive* (fully unintegrated) NLO evolution kernels are required in order to impose NLO corrections within a simpler LO MC parton shower, by means of reweighting the LO distribution, as

* Presented by Magdalena Slawinska at the Cracow Epiphany Conference on the First Year of the LHC, Cracow, Poland, January 10–12, 2011.

** This work is supported by the Polish Ministry of Science and Higher Education grant No. 1289/B/H03/2009/37.

outlined in Ref. [3][1]. In this method the LO MC parton shower has to be reconstructed from the scratch, contrary to methodology of Ref. [11], where at the price MC weights being non-positive, one is able to use standard LO parton shower MC.

Very schematically, the corresponding MC weight reads

$$\text{MC weight} = \frac{\text{exact NLO diagram distribution}}{\text{crude LO distribution}}\,. \tag{1}$$

The potential problem is that a single Feynman diagram, or small subset of diagrams, entering the exclusive NLO kernel (and the MC weight) generally is not gauge-invariant and may feature uncancelled soft singularities. The Monte Carlo weights may then explode, unless the *crude* distributions of the LO MC already reproduces exactly soft singularities of NLO diagrams. It is therefore very important to understand, in fine detail, the structure of soft and collinear singularities in exclusive kernels, as implemented in LO MC including also complete NLO corrections.

For the purpose of the MC we are going to analyse the example diagrams and their groups one by one, gaining the detailed knowledge about the structure of collinear and soft singularities of each Feynman diagram contributing to the NLO kernel and the interplay between diagrams. We shall exploit tools and methods of the graphical analysis of the infra-red singularities which were already used for the non-singlet diagrams in Ref. [12]. Here, we will extend this study to a gauge invariant subset of two-real singlet diagrams contributing to the P_{gq} NLO DGLAP kernel. Let us stress that the cancellations discussed in the following are not of the usual KLN [13] nature, *i.e.* between the real and virtual Feynman diagrams, but rather among the real diagrams alone, and are governed by the spin and colour quantum numbers. The contributions of the diagrams to the standard DGLAP (inclusive) kernels analysed in the following have been already defined and used in Refs. [14] and [15]. Generally, we shall examine the structure of the soft and collinear singularities of the unintegrated distributions related to these NLO DGLAP evolution kernels.

2. Singlet diagrams considered

The singlet diagrams considered in this contribution originate from the LO amplitude for splitting a gluon into quark (antiquark)

[1] In the complementary approach of Refs. [8,9,10] soft singularities are resummed first and collinear resummation is added next.

by means of adding the NLO corrections from the emission of an additional gluon

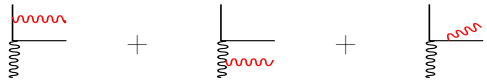

Feynman diagrams contributing to the NLO kernel result from squaring the above sum of amplitudes and are displayed in Fig. 1. It is worth noting, that the ladder diagrams (the first and the third in the upper row in Fig. 1) enter the NLO kernel supplemented with the so-called collinear counterterms that subtract off the leading-order contributions. In this contribution, however, the counterterms will be included only at the end of the analysis, and before that the leading-order singularities will be visible.

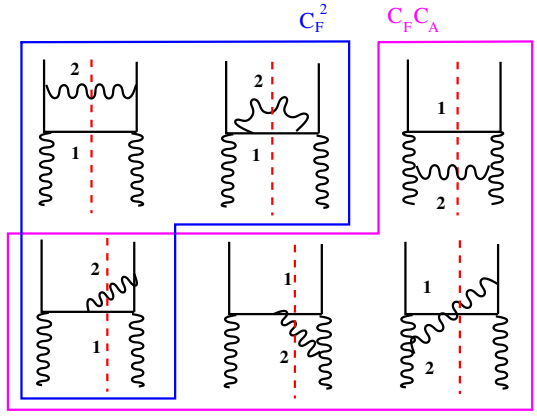

Fig. 1. Singlet gluon–quark diagrams; "1" denotes a quark and "2" — a gluon.

We will adopt the same approach as in Ref. [12] and analyse all distributions in the logarithmic Sudakov variables $(\ln(a_1/a_2), \ln(\alpha_1/\alpha_2))$, where α_i come from the Sudakov parametrisation of four-momenta of the emitted particles: $k_i = \alpha_i p + \alpha_i^- n + k_{i\perp}$ and a_i are angular (rapidity-related) variables, $a_i = \frac{|\overrightarrow{k_{i\perp}}|}{\alpha_i}$. All contributions are normalised to the eikonal phase space

$$d\Psi = \frac{d\alpha_1}{\alpha_1}\frac{d\alpha_2}{\alpha_2}\frac{da_1}{a_1}\frac{da_2}{a_2}, \tag{2}$$

with the angles integrated over. Moreover, we will ensure that at least one emission is hard by constraining $\alpha_1+\alpha_2 = 1-x > 0$. Similarly, the maximal angle is fixed to an arbitrary parameter. Hence, the ratios a_1/a_2 and α_1/α_2 will measure the relative hardness and angles of the two partons.

We will explore the soft limit of the diagrams in Fig. 1, namely the limit where both $|\overrightarrow{k_{\mathrm{T}_i}}| \to 0$ and $\alpha_i \to 0$ (for a given i), but a_i remains finite. In

the logarithmic Sudakov variables the singularities will appear on the plots as one- or two-dimensional infinite structures.

3. Results

Let us first consider the C_{F}^2 diagrams, corresponding to emission of a gluon from a quark. The bremsstrahlung type diagram is displayed in Fig. 2, left. It has a doubly-logarithmic singularity visible as the infinite trapezoidal plateau, bordered by the lines $\alpha_1 = \alpha_2$ and $\frac{a_2^2}{a_1^2} = \frac{\alpha_1}{\alpha_2}$ (the line of equal "minus lightcone variables" α_i^-). The second diagram, representing the amplitude-squared of emission of a gluon from the emitted quark (Fig. 2, middle), features a collinear singularity manifesting itself as the infinite ridge along the line of equal angles. This singularity, however, is not related to the soft limit (it is compensated by the virtual diagram) and will not be considered here. This diagram has also a doubly-logarithmic singularity in the form of a triangular plateau, bordered by the lines of equal angles and "minus variables". The sum of the two (the rightmost plot in Fig. 2) features two equal-height plateaux with the canyon at the line of equal minus variables.

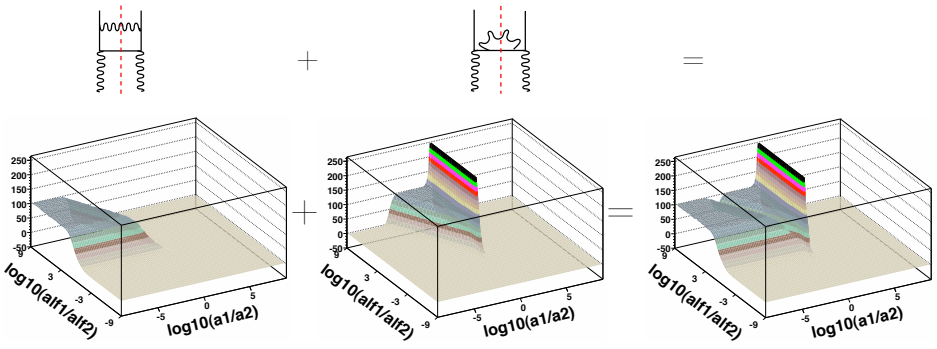

Fig. 2. Amplitude-squared diagrams $\sim C_{\mathrm{F}}^2$.

The most singular terms from the distributions of the diagrams are necessarily proportional to the products of the leading-order DGLAP kernels

$$\approx C_{\mathrm{F}}^2 \frac{\left(\alpha_1^2 + (1-\alpha_1)^2\right)\left(x^2 + (1-\alpha_1)^2\right)}{\alpha_1 \alpha_2^2} \frac{a_2^4}{q^4(a_1, a_2)} \tag{3}$$

and

$$P_{qg}(z_1) P_{qq}(z_2) = C_{\mathrm{F}}^2 \frac{\alpha_1^2 + (1-\alpha_1)^2}{2} \frac{x^2 + (1-\alpha_1)^2}{(1-\alpha_1)\alpha_2}\,, \tag{4}$$

where $z_1 = 1 - \alpha_1$ and $z_2 = \frac{x}{1-\alpha_1}$. Similarly

$$\approx 2C_{\rm F}^2 \frac{\alpha_1 \left(x^2 + (1-x)^2\right)}{\alpha_2^2} \frac{a_1^4 a_2^2}{a^2} \frac{1}{q^4(a_1, a_2)}\,, \tag{5}$$

$$P_{qg}(z_1)P_{qq}(z_2) = C_{\rm F}^2 \frac{x^2 + (1-x)^2}{2} \frac{(1-x)^2 + \alpha_1^2}{(1-x)\alpha_2}$$
$$\xrightarrow[\alpha_2 \to 0]{} C_{\rm F}^2 \left(x^2 + (1-x)^2\right) \frac{\alpha_1}{\alpha_2}\,, \tag{6}$$

where $z_1 = 1 - x$ and $z_2 = \frac{\alpha_1}{1-x}$.

In (3) and (6) we also used $q^2(a_1, a_2) = \frac{1-\alpha_2}{\alpha_2} a_1^2 + \frac{1-\alpha_1}{\alpha_1} a_2^2 + 2a_1 a_2 \cos\phi$ (the denominator of the most virtual quark) and $a^2 = a_1^2 + a_2^2 - 2a_1 a_2 \cos\phi$ (proportional to the invariant mass of the emitted quark and gluon).

The "canyon" structure in the plot, being the remaining singly-logarithmic singularity, however, spoils the soft limit regardless of the counterterm employed. If we add now the interference diagram[2], as shown in Fig. 3, the canyon gets removed.

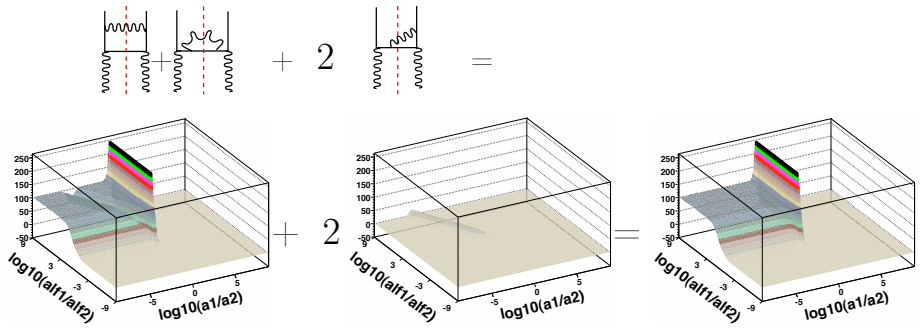

Fig. 3. The infra-red cancellations among the diagrams $\sim C_{\rm F}^2$.

What remains is the uniform plateau bordered by $a_1 = a_2$ collinear singularity. The "minus variable" ordering, preferred by each diagram separately, turns out to be irrelevant for the sum of diagrams!

From the above formulae it follows that the quadratic plateau represents the leading-order contribution. In the NLO kernel it is removed by the counterterm of the factorisation procedure equal to

$$C^{C_{\rm F}^2} = 4C_{\rm F}^2 \frac{\left(x^2 + (1-\alpha_1)^2 \left(\alpha_1^2 + (1-\alpha_1)^2\right)\right)}{\alpha_1 \alpha_2^2 (1-\alpha_1)^2 (1-\alpha_2)} \frac{1}{a_1^2 a_2^2}\,. \tag{7}$$

[2] This diagram's colour coefficient is equal to $C_{\rm F}^2 - C_{\rm A}C_{\rm F}/2$. In this analysis we add only its part $\sim C_{\rm F}^2$, adding the other one $\sim -C_{\rm A}C_{\rm F}/2$ to the $C_{\rm A}C_{\rm F}$ diagrams.

The doubly logarithmic singularity of the counterterm depends on the details of factorisation procedure in use[3].

The $C_A C_F$ subset consists of diagrams that correspond to the emission of a gluon from the incoming gluon. They include only one amplitude-squared diagram. Displayed in Fig. 4, left, it has a doubly-logarithmic singularity — the plateau stretching in the two regions: where the angle of the emitted gluon is larger than the quark's and *vice versa*. The diagram contributes in the region of phase space where both emissions are ordered in the minus variable. After adding to the interference diagram, the boundaries of the resulting plateau are corrected and the sum contributes in the region of the phase space, where the angle of the quark is larger than angle of the gluon.

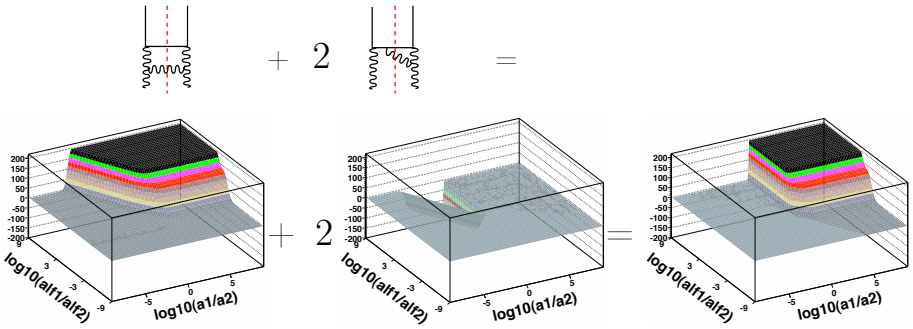

Fig. 4. The cancellation of doubly-logarithmic singularities among diagrams $\sim C_F C_A$.

The collinear counterterm is given by

$$C^{C_A C_F} = 2 C_A C_F \frac{\left(\alpha_1^2 + x^2\right)\left(4\alpha_2^3 - \alpha_2^2 - 3\alpha_2 + 4\right)}{\alpha_1 \alpha_2^2 (1-\alpha_1)^3} \frac{1}{a_1^2 a_2^2} \,. \tag{8}$$

While the C_F^2 counterterm of Eq. (7) features the $a_1 < a_2$ ordering, the ordering in the $C_A C_F$ counterterm of Eq. (8) is the opposite ($a_2 < a_1$) due to a gluon being emitted before a quark.

The remaining $C_A C_F$ interferences feature single-log singularities, seen as infinite canyons/ridges along the line of equal minus-variables in Fig. 5 that cancel out when added. What remains is the little hill in the central region, which leads to a finite contribution.

The sum of all singlet diagrams discussed in this contribution is presented in Fig. 6. The left-hand side plot in this figure shows two leading-order

[3] The counterterm in Eq. (7) has additional theta function related to ordering of the emissions (not shown explicitly), defining the boundaries of the LO plateaux. In the following we will use the ordering in the angular variables a.

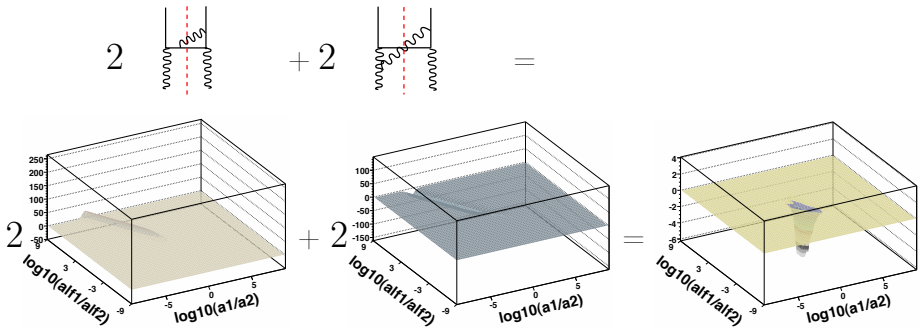

Fig. 5. The cancellation of singly-logarithmic singularities among interference diagrams $\sim C_{\mathrm{F}}C_{\mathrm{A}}$.

plateaux separated by the line of equal angles $a_1 = a_2$. The line represents a collinear singularity and comes from the diagram, in which the additional gluon is emitted from the emitted quark. The plateau on the left (in brown) corresponds to the topologies in which a soft gluon is emitted from a quark. The right-hand side plateau (navy-blue) represents contributions with a soft gluon emitted from the incoming gluon. The relative height of both plateaux is equal to $C_{\mathrm{F}}^2/C_{\mathrm{F}}C_{\mathrm{A}}$, as expected.

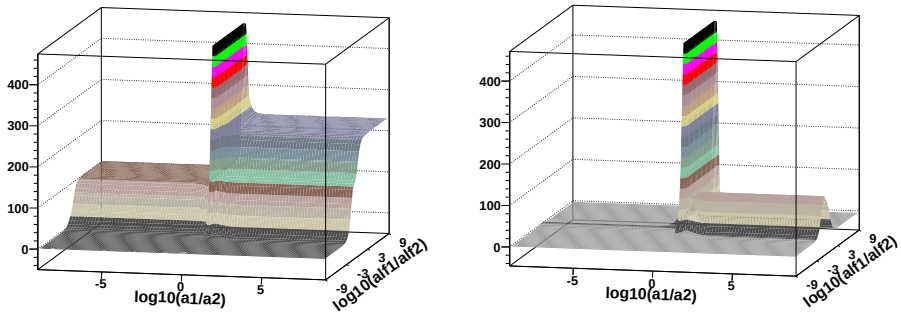

Fig. 6. All singlet gluon–quark contributions to the NLO kernel added together (left) and with counterterms subtracted (right).

In the right plot the same sum is presented, but with the leading order singularities cancelled out by the factorisation counterterms of Eqs. (7) and (8) on the left- and right-hand side of this plot, respectively. The plot features the collinear singularity only.

4. Conclusions

We conclude that the restoration of gauge invariance (colour coherence) is crucial in cancelling infra-red singularities. We understand the soft limits of NLO exclusive kernels, observe and explain the cancellations of double- and single-logarithmic soft singularities. The angular ordering is the preferred parametrisation of the phase space in view of the soft singularity structure of the distributions from gauge-invariant subset of diagrams contributing to NLO evolution kernels in the exclusive (unintegrated) form.

REFERENCES

[1] S. Jadach, M. Skrzypek, A. Kusina, M. Slawinska, *PoS* **RADCOR2009**, 069 (2010) [arXiv:1002.0010v1 [hep-ph]].

[2] S. Jadach, A. Kusina, M. Skrzypek, M. Slawinska, arXiv:1102.5083v1 [hep-ph].

[3] S. Jadach *et al.*, arXiv:1103.5015v1 [hep-ph].

[4] L.N. Lipatov, *Sov. J. Nucl. Phys.* **20**, 95 (1975); V.N. Gribov, L.N. Lipatov, *Sov. J. Nucl. Phys.* **15**, 438 (1972); G. Altarelli, G. Parisi, *Nucl. Phys.* **126**, 298 (1977); Yu.L. Dokshitzer, *Sov. Phys. JETP* **46**, 64 (1977).

[5] R.K. Ellis *et al.*, *Phys. Lett.* **B78**, 281 (1978).

[6] G. Curci, W. Furmanski, R. Petronzio, *Nucl. Phys.* **B175**, 27 (1980).

[7] M. Botje, *Comput. Phys. Commun.* **182**, 490 (2011) [arXiv:1005.1481v3 [hep-ph]].

[8] B.F.L. Ward, *Ann. Phys.* **323**, 2147 (2008) [arXiv:0707.3424v2 [hep-ph]].

[9] S. Joseph, S. Majhi, B.F.L. Ward, S.A. Yost, *Phys. Lett.* **B685**, 283 (2010) [arXiv:0906.0788v4 [hep-ph]].

[10] S. Joseph, S. Majhi, B.F.L. Ward, S.A. Yost, *Phys. Rev.* **D81**, 076008 (2010) [arXiv:1001.1434v2 [hep-ph]].

[11] S. Frixione, B.R. Webber, *J. High Energy Phys.* **06**, 029 (2002) [arXiv:hep-ph/0204244v2].

[12] M. Slawinska, A. Kusina, *Acta Phys. Pol. B* **40**, 2097 (2009) [arXiv:0905.1403v1 [hep-ph]].

[13] T. Kinoshita, *J. Math. Phys.* **3**, 650 (1962); T.D. Lee, M. Nauenberg, *Phys. Rev.* **B133**, 1549 (1964).

[14] W. Furmanski, R. Petronzio, *Phys. Lett.* **B97**, 437 (1980).

[15] R.K. Ellis, W. Vogelsang, arXiv:hep-ph/9602356v1.